Supplementary material

Revealing the mass transfer of proton donors for tailoring hydrogen evolution coupled with manganese electrodeposition

Cai Tan[a], Chaoyi Chen[a,b*], Fan Yang[a,b*], Junqi Li[a], Liangxing Jiang[c],Changping Shi[a], Jiangyuan Yang[a], Yuanyu Chen[a], Lu Yu[a],

[a]College of Materials and Metallurgy, Guizhou University, Guiyang, Guizhou, 550025, China

[b]Guizhou Province Dual Carbon and New Energy Technology Innovation and Development Research Institute, Guiyang 550025, China

[c]School of Metallurgy and Environment, Central South University, Changsha, Hunan 410083, China

[*] Corresponding author

E-mail address: ccy197715@126.com; fyang7@gzu.edu.cn

This file includes:

Supplementary Notes 1 to 7

Supplementary Figures 1 to 10

Supplementary Tables 1 to 6

Supplementary References 1 to 5

Table of Contents

1. Supplementary Notes

In-situ Raman spectroelectrochemical investigation

In situ Raman spectra were recorded on a LabRAM HR Evolution (HORIBA Scientific) spectrometer with a He-Ne laser (wavelength λ=532 nm), 50× objective, and 600 lines mm^{-1} grating. The 50% laser intensity for 120s with two sweeps per spectrum was used to attenuate the absorption of the Raman signal by the liquid and obtain a good signal-noise ratio (SNR). A Pt wire and a saturated Hg/Hg_2O electrode (saturated M KCl as inner filling electrolyte) were applied as the counter electrode and the reference electrode, respectively. The electrochemical conditions were maintained by applying a constant potential of 0~2.0 V using an electrochemistry workstation.

The cathode current efficiency and DC power consumption

Galvanostatic electrowinning was carried out at a current density of 400·A·m^{-2} (maintained for 1 hour at a temperature of 30 ° C). The electrolyte was composed of 20 g/L $MnSO_4 \cdot H_2O$ and 130 g/L $(NH_4)_2SO_4$ (the results are shown in Figure 1e). After the end of electrolysis, the cathode is placed in a vacuum drying tank and dried at 60 °C for 12 h. After the electrode is cooled to room temperature, the change of cathode mass (Δm) is measured, and the cathode current efficiency (CE) and DC power consumption (EC) are calculated according to (Eq. S1) and (Eq. S2), respectively.

$$CE = \frac{\mathrm{V}mz\mathrm{F}}{It\mathrm{M}_{\mathrm{Mn}}} \times 100\% \quad \text{(Eq. S1)}$$

$$EC = \frac{Q_{Mn} \times U}{CE} \quad \text{(Eq. S2)}$$

Where I is the current intensity; t is time; and M_{Mn} is the relative atomic mass of Mn, U is the trough voltage; Q_{Mn} is the theoretical power consumption of manganese precipitation.

The electrochemical impedance spectroscopy

The fitting data (dots) were obtained by fitting experimental data (lines) using Armstrong equivalent circuits (Figure S2). Where the constant phase element (CPE_{dl}) replaces the capacitive element (C_{dl}) in the fitting process, *Rs* represents the sum of electrode internal resistance and electrolyte resistance, C_{dl} represents the double-layer capacitor, R_1 represents the desorption resistance of $H_{ads,}$ R_2, and CPE_{dl} represent the adsorption resistance and the corresponding capacitance, and the resistance of the constant phase element is calculated by Eq. S3.

$$Z_{CPE} = \frac{1}{Q(jw)^n} \quad \text{(Eq. S3)}$$

Q is the double-layer capacitor; j is the arithmetic square root of -1; ω is the angular frequency, n characterizes the deviation between the electrode surface and the ideal parallel double layer.

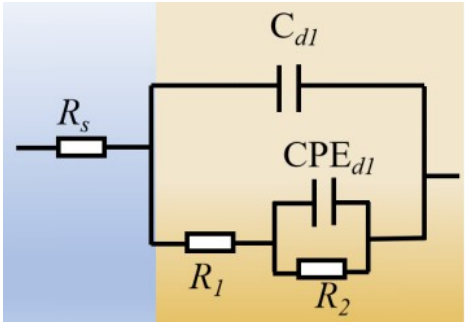

Figure S1 Diagram of Armstrong equivalent circuit

The activation energy

Figure S5 shows the linear sweep voltammetry (LSV) curves of HER at 25 °C, 30 °C, 35 °C, 40 °C, and 45 °C, it can be seen that the current increases with the increase of temperature during the electrolysis process, in this work, the apparent activation energy of HER can obtain from the classical Arrheniusis (Eq. S4) [1]:

$$\ln(j) = \ln A + \frac{E_{\mathrm{a}}}{\mathrm{RT}} \qquad \text{(Eq. S4)}$$

Where R is the molar gas constant, j is the current density, and A and E_a are two empirical parameters, called the anterior parameter and the activation energy, respectively.

The Tafel slope

The Overpotential (η_{HER}) of HER was corrected by fitting experimental data in equation S5, then the Tafel slope can be obtained by plotting current density (log (i) vs overpotential (η_{HER}).

$$\eta_{HER} = E - iR - \left(\mathrm{E}^{\theta}_{H^+/H} + \frac{2.303\mathrm{RT}}{\mathrm{ZF}} \log C_{H^+} \right) \qquad \text{(Eq. S5)}$$

Where R is the solution resistance between the reference electrode and the working electrode, and $E_{H^+/H}^{\theta}$ and C_{H^+} are the standard electrode potential of the H^+/H electric pair and the H^+ concentration of the bulk solution, respectively.

The density functional theory calculations

The adsorption energy of PDs and Gibbs free energy of HER are considered, in this study, and the possible reaction pathway of the HER (Including Volmer, Heyrovsky, and Tafel reaction pathway) in the neutral solution is as follows:

1) H_2O

the alkaline Volmer reaction pathway:

$$*+H_2O=*H_2O$$

$$*H_2O+e^-=*H_{ads}+*OH^-$$

the alkaline Heyrovsky reaction pathway:

$$*H_{ads}+H_2O=*H_{ads}+*H_2O$$

$$*H_{ads}+*H_2O+e^-=*H_2+*OH^-$$

the alkaline Tafel reaction pathway:

$$*H_{ads}+*H_{ads}=*H_2$$

$$*H_2=H_2$$

2) NH_4^+

the alkaline Volmer reaction pathway:

$$*+NH_4^+=*NH_4^+$$

$$*NH_4^++e^-=*NH_3+*H_{ads}$$

the alkaline Heyrovsky reaction pathway:

$$*H_{ads}+NH_4^+=*H_{ads}+*NH_4^+$$

$$*H_{ads}+*NH_4^++e^-=*NH_3+*H_{ads}$$

For the free energy calculations of each step mentioned above, a correction is applied by computing the frequencies of surface-adsorbed molecules [2, 3]. The corrected free energy is calculated as follows：

$$\Delta G = \Delta E - \Delta ZPE - \mathrm{T}\Delta S + \Delta G_U$$

Here, ΔZPE represents the zero-point vibrational energy, TΔS is the entropy correction,

and ΔG_U is equal to eU, where U is the mentioned potential of 0 V.

Dynamics simulation of hydrogen evolution

The study has proposed that H_2O rather than H^+ is the reactant of HER in an alkaline/neutral environment, which directly dissociates on the surface of the electrode [4]. However, in the presence of multiple proton donors, not only water molecules at the electrolyte interface can participate in HER, but also other proton donors (such as HPO_4^-, NH_4^+) [5]. Therefore, with consideration of the presence of multiple proton donors (H_2O, NH_4^+), a microkinetic model for HER in a neutral environment was constructed as shown in Tables S3~S6, which list the elementary reaction steps and the enrolled reaction rate equations of HER in a neutral electrolyte. where r is the elementary reaction rate [$mol \cdot m^{-2} \cdot s^{-1}$], K is the reaction rate constant [$mol \cdot m^{-2} \cdot s^{-1}$], c is the concentration [$mol \cdot m^{-3}$], α is the symmetry coefficient, η is the overpotential [V], R is the molar gas constant [$J \cdot mol^{-1} \cdot K^{-1}$], T is the temperature [K], θ is the coverage, θ subscripts H_{ads} represent the activated of adsorbed H intermediate.

2. Supplementary figures

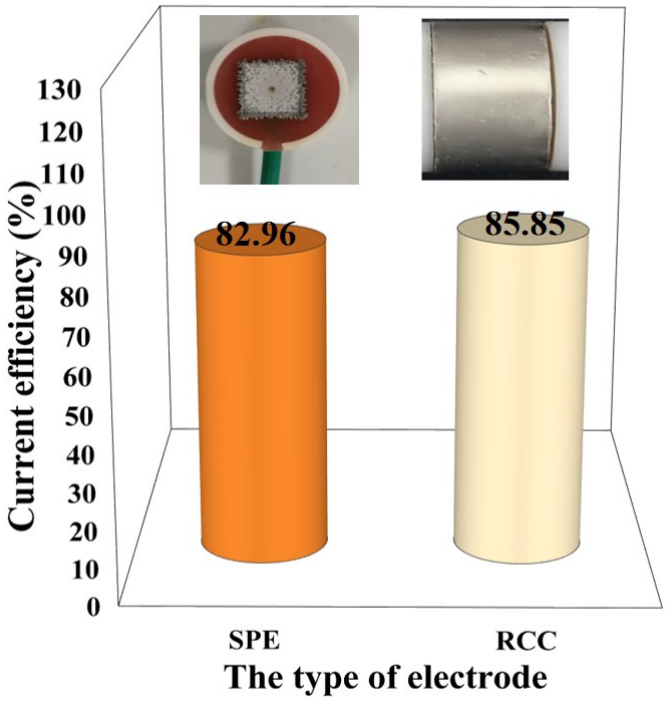

Figure S2 CE of Mn electrodeposition on SPE and RCC

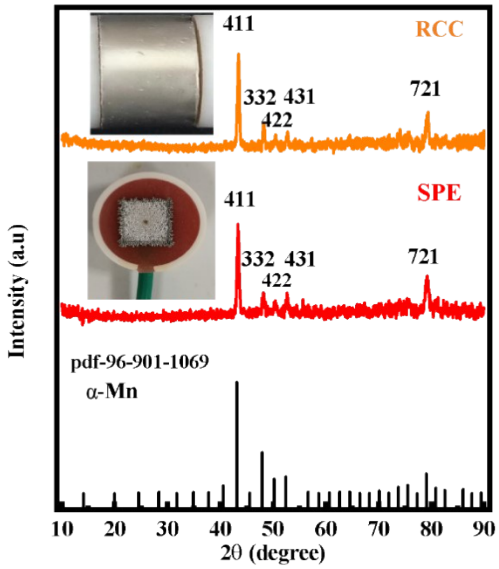

Figure S3 X-ray diffraction of SPE and RCC

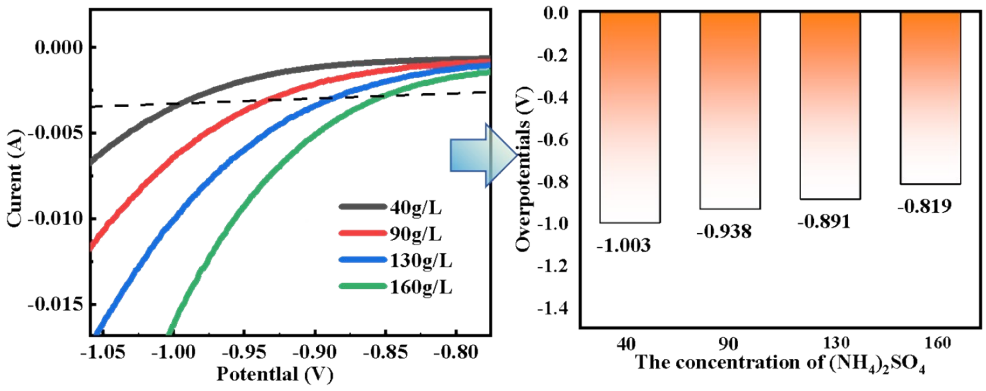

Figure S4 LSV and corresponding overpotential of HER on RCC (1000 rpm, 30 ℃)

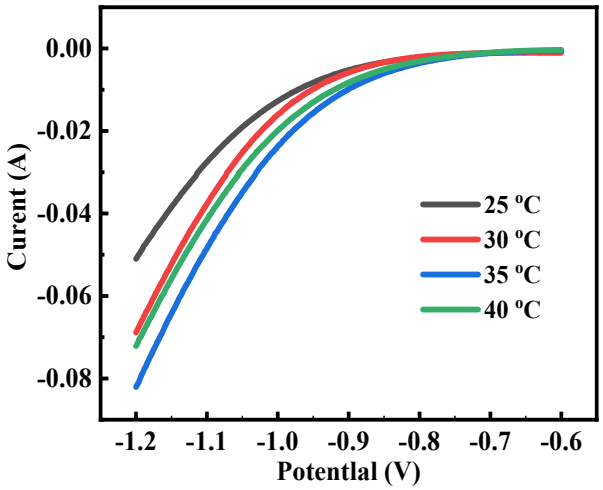

Figure S5 LSV curves of HER on RCC (130 g/L $(NH_4)_2SO_4$, 1000 rpm)

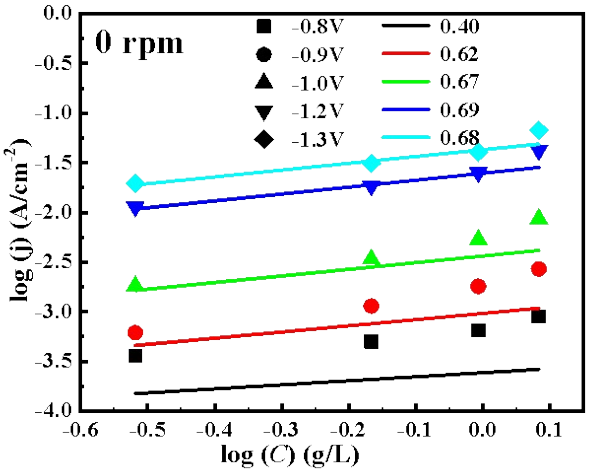

Figure S6 Order of reaction on RCC at -0.8~-1.3 V potential (0 rpm)

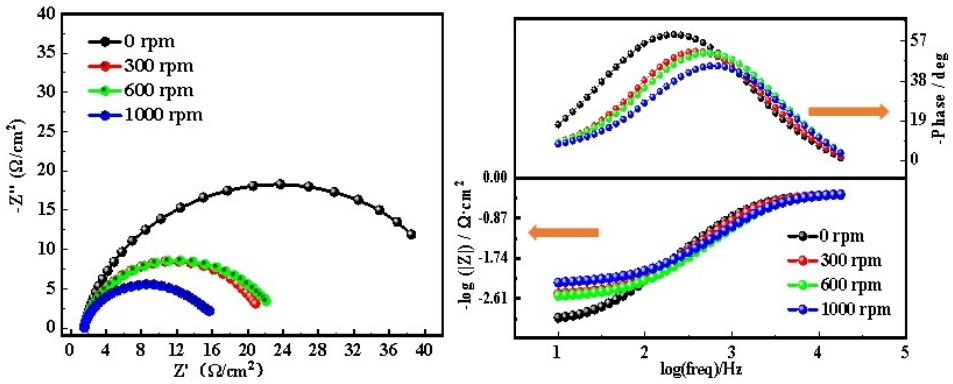

Figure S7 EIS of HER on RCC (130 g/L $(NH_4)_2SO_4$, 30 ℃)

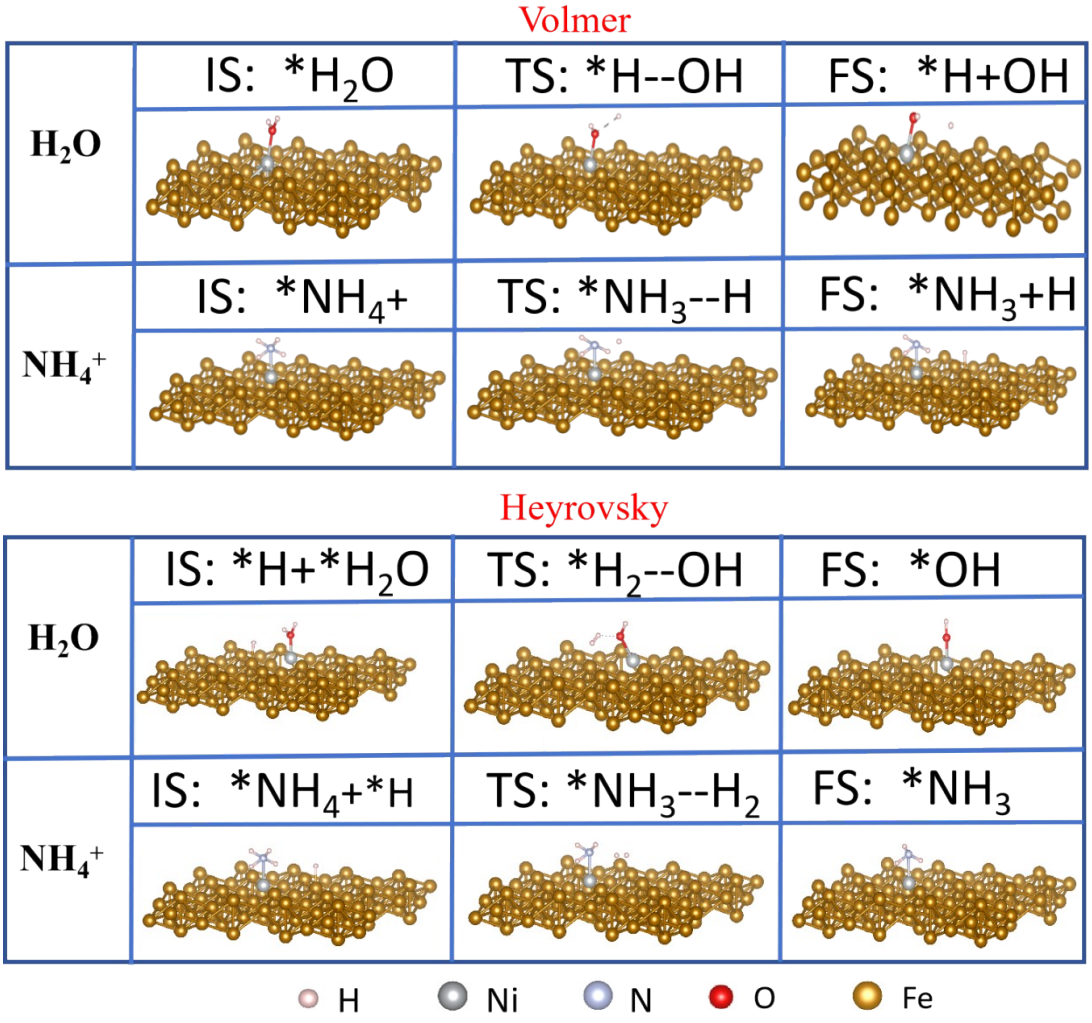

Figure S8 Minimum energy path (MEP) of the Volmer and Heyrovsky reaction of H_2O and NH_4^+

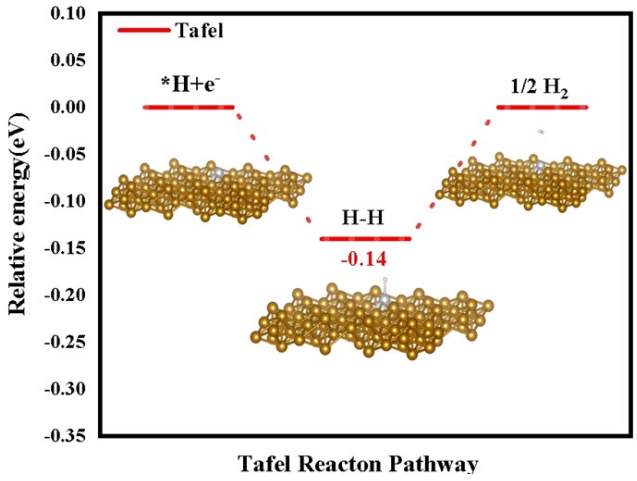

Figure S9 Relative energy along the Tafel reaction pathway

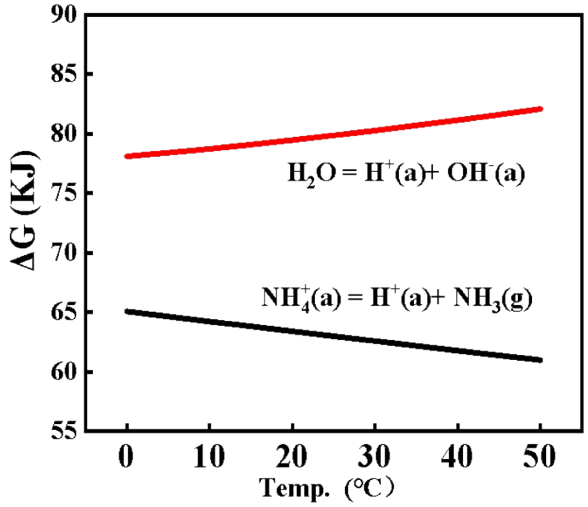

Figure S10 Gibbs free energy of the reaction H_2O and NH_4^+

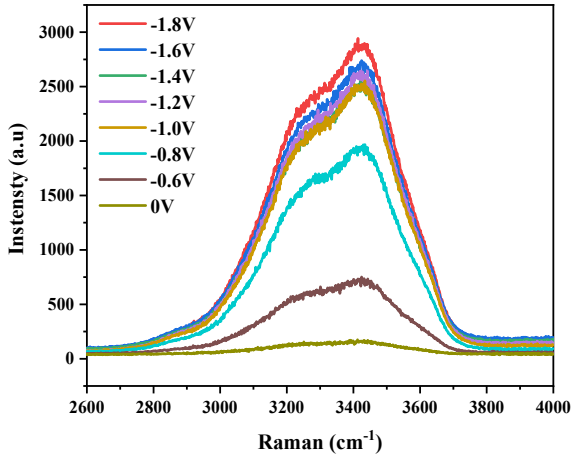

Figure S11 In-situ Raman tests of HER in the H_2O-130g/L$(NH_4)_2SO_4$ at -0.2~-1.8V

potentials

3. Supplementary tables

Table S1 The fitting Tafel constants of HER on RCC corresponding to Figure 2b

	$C(NH_4)_2SO_4$	a	b	β	$\log(i_0)$
30℃	40 (g/L)	2.64	0.63	0.09	-4.01
	90 (g/L)	1.72	0.41	0.15	-4.22
1000 rpm	130 (g/L)	1.18	0.25	0.24	-4.66
	160 (g/L)	1.16	0.25	0.23	-4.51

Table S2 The EIS of HER on RCC corresponding to Figure 2d

Concentration (g/L)	Rs (Ω/cm^2)	C_{d1} ($\mu F/cm^2$)	R_1 (Ω/cm^2)	CPE_{dl} ($\mu F/cm^2$)	n /	R_2 (Ω/cm^2)
40	7.11	26.27	21.70	42.43	0.89	158.10
90	4.25	16.04	15.52	61.62	0.90	61.15
130	3.44	33.96	15.14	61.24	0.94	26.22
160	2.19	43.61	12.23	225.9	0.96	5.16

1

2 **Tabel S3** The elementary reaction steps of HER with VHT on RCC

VHT	H_2O and NH_4^+ are the main proton donor	
Reaction steps	V: $\frac{1}{2}NH_4^+ + \frac{1}{2}H_2O + e^- M \cdot H_{ads} + \frac{1}{2}OH^- + \frac{1}{2}NH_3 \underset{k_{-1}}{\overset{k_1}{\rightleftharpoons}}$	(Eq. S6)
	H: $H_{ads} + \frac{1}{2}H_2O + \frac{1}{2}H^+ + e^- H_2 + \frac{1}{2}OH^- \underset{k_{-2}}{\overset{k_2}{\rightleftharpoons}}$	(Eq. S7)
	T: $2M \cdot H_{ads} H_2 \underset{k_{-3}}{\overset{k_3}{\rightleftharpoons}}$	(Eq. S8)
Reaction rate ($mol \cdot m^{-2} \cdot s^{-1}$)	$r_1 = k_1 \cdot \left(1 - \theta_{H_{ads}}\right) \cdot \left(\frac{C_{NH_4^+}}{C^\Theta}\right)^{1/2} \cdot exp\left(\frac{\alpha_1 F\eta}{RT}\right)$	(Eq. S9)
	$r_{-1} = k_{-1} \cdot \theta_{H_{ads}} \cdot \left(\frac{C_{OH^+}}{C^\Theta}\right)^{1/2} \cdot exp\left(-\frac{(1-\alpha_1)F\eta}{RT}\right)$	(Eq. S10)
	$r_2 = k_2 \cdot \theta_{H_{ads}} \cdot \left(\frac{C_{H^+}}{C^\Theta}\right)^{1/2} \cdot exp\left(\frac{\alpha_2 F\eta}{RT}\right)$	(Eq. S11)
	$r_{-2} = k_{-2} \cdot \left(1 - \theta_{H_{ads}}\right) \cdot \left(\frac{C_{OH^+}}{C^\Theta}\right)^{1/2} \cdot exp\left(-\frac{(1-\alpha_2)F\eta}{RT}\right)$	(Eq. S12)
	$r_3 = k_3 \theta^2_{Hads}$	(Eq. S13)
	$r_{-3} = k_{-3}\left(1 - \theta^2_{Hads}\right)$	(Eq. S14)
Reaction rate equations	$C_{H_{ads}} \frac{d\theta_{H_{ads}}}{dt} = r_1 - r_{-1} - r_2 + r_{-2} - r_3 + r_{-3}$	(Eq. S15)
	$C\frac{dE}{dt} = j(t) - \frac{(r_1 - r_{-1} + r_2 - r_{-2})F}{n}$	(Eq. S16)

3

4

1 **Tabel S4** The elementary reaction steps of HER with VH on RCC

VH	H_2O and NH_4^+ are the main proton donor	(Eq. S17)
Reaction steps	V: $\frac{1}{2}NH_4^+ + \frac{1}{2}H_2O + e^- M \cdot H_{ads} + \frac{1}{2}OH^- + \frac{1}{2}NH_3$ 	(Eq. S18)
	H: $M \cdot H_{ads} + \frac{1}{2}H_2O + \frac{1}{2}H^+ + e^- H_2 + \frac{1}{2}OH^-$	(Eq. S19)
Reaction rate ($mol \cdot m^{-2} \cdot s^{-1}$)	$r_1 = k_1 \cdot \left(1 - \theta_{H_{ads}}\right) \cdot \left(\frac{C_{NH_4^+}}{C^\Theta}\right)^{1/2} \cdot exp\left(\frac{\alpha_1 F\eta}{RT}\right)$	(Eq. S20)
	$r_{-1} = k_{-1} \cdot \theta_{H_{ads}} \cdot \left(\frac{C_{OH^+}}{C^\Theta}\right)^{1/2} \cdot exp\left(-\frac{(1-\alpha_1)F\eta}{RT}\right)$	(Eq. S21)
	$r_2 = k_2 \cdot \theta_{H_{ads}} \cdot \left(\frac{C_{H^+}}{C^\Theta}\right)^{1/2} \cdot exp\left(\frac{\alpha_2 F\eta}{RT}\right)$	(Eq. S22)
	$r_{-2} = k_{-2} \cdot \left(1 - \theta_{H_{ads}}\right) \cdot \left(\frac{C_{OH^+}}{C^\Theta}\right)^{1/2} \cdot exp\left(-\frac{(1-\alpha_2)F\eta}{RT}\right)$	(Eq. S23)
Reaction rate equations	$C_{H_{ads}} \frac{d\theta_{H_{ads}}}{dt} = r_1 - r_{-1} - r_2 + r_{-2}$	(Eq. S24)
	$C\frac{dE}{dt} = j(t) - \frac{(r_1 - r_{-1} + r_2 - r_{-2})F}{n}$	(Eq. S25)

2

3

Tabel S5 The elementary reaction steps of HER with VT on RCC

VT	H_2O and NH_4^+ are the main proton donor	(Eq. S26)
Reaction steps	V: $\frac{1}{2}NH_4^+ + \frac{1}{2}H_2O + e^- M \cdot H_{ads} + \frac{1}{2}OH^- + \frac{1}{2}NH_3$	(Eq. S27)
	T: $M \cdot H_{ads} \frac{1}{2}H_2$	(Eq. S28)
Reaction rate ($mol \cdot m^{-2} \cdot s^{-1}$)	$r_1 = k_1 \cdot \left(1 - \theta_{H_{ads}}\right) \cdot \left(\frac{C_{NH_4^+}}{C^\Theta}\right)^{1/2} \cdot exp\left(\frac{\alpha_1 F\eta}{RT}\right)$	(Eq. S29)
	$r_{-1} = k_{-1} \cdot \theta_{H_{ads}} \cdot \left(\frac{C_{OH^+}}{C^\Theta}\right)^{1/2} \cdot exp\left(-\frac{(1-\alpha_1)F\eta}{RT}\right)$	(Eq. S30)
	$r_2 = k_2 \theta^2_{Hads}$	(Eq. S31)
	$r_{-2} = k_{-2}(1 - \theta_{Hads})^2$	(Eq. S32)
Reaction rate equation	$C_{H_{ads}} \frac{d\theta_{H_{ads}}}{dt} = r_1 - r_{-1} - r_2 + r_{-2}$	(Eq. S33)
	$C\frac{dE}{dt} = j(t) - \frac{(r_1 - r_{-1})F}{n}$	(Eq. S34)

There, r is the elementary reaction rate [mol·m^{-2}·s^{-1}]; K is the reaction rate constant [mol·m^{-2}·s^{-1}]; C is the concentration [mol·m^{-3}]; θ is the coverage; α is the symmetry coefficient; η is the overpotential [V]; R is the gas constant, 8.314 [J·mol^{-1}·K^{-1}]; T is the temperature [K].

1 **Tabel S6** The rate constants of HER on RCC corresponding to **Figure 5**

model	speed (rpm)	k_1	k_{-1}	k_2	k_{-2}	k_3	θ_{Hads}	R^2
VHT	0	5.81×10^{-6}	2.22×10^{-9}	0.5005	4.52×10^{-7}	0.007	0.57	0.9999
	1000	7.96×10^{-2}	8.77×10^{-9}	0.9576	1.66×10^{-10}	1.098	0.29	0.9877
VH	0	1.48×10^{-4}	2.08×10^{-5}	0.9630	1.13×10^{-6}		5.90×10^{-3}	0.9811
	1000	9.41×10^{-1}	0.24×10^{-6}	0.9938	3.26×10^{-8}		1.06×10^{-5}	0.9999
VT	0	0.63	9.14×10^{-3}	0.8990	0.59×10^{-6}		1.27×10^{-7}	0.9824
	1000	0.69	1.78×10^{-8}	0.9117	0.73×10^{-6}		6.26×10^{-9}	0.9879

2

4. Supplementary References

[1] R. Creţu, A. Kellenberger, N. Vaszilcsin, Enhancement of hydrogen evolution reaction on platinum cathode by proton carriers[J], International Journal of Hydrogen Energy 2013, 38(27), 11685-11694.

[2] Kresse, G.; Joubert, D. From ultrasoft pseudopotentials to the projector augmented-wave method[J]. Physical Review B 1999, 59, 1758-177.

[3] Perdew, J. P.; Burke, K.; Ernzerhof, M. Generalized gradient approximation made simple[J]. Physical Review Letters 1996, 77, 3865-3868.

[4] Subbaraman, R., et al. Enhancing hydrogen evolution activity in water splitting by tailoring Li^+ -$Ni(OH)_2$-Pt interfaces[J]. *Science* 2011, 334, 1256-1260.

[5] Jackson M N , Jung O , Lamotte H C ,et al. Donor-Dependent Promotion of Interfacial Proton-Coupled Electron Transfer in Aqueous Electrocatalysis[J]. ACS Catalysis, 2019, 9(4).